SENSITIVITY ANALYSIS OF CONCRETE PERFORMANCE USING FINITE ELEMENT APPROACH

Y. H. Parjoko

Directorate General of Highway Construction, Minsitry of Public Works, Republic of Indonesia
Email: hendrik_gor78@yahoo.com

ABSTRACT

This study aims to understand the effect of applying several parameters: different axle load configuration, concrete properties, subgrade properties, slab thickness, joint characteristics, shoulder construction, bounded HMA overlay on concrete pavement, and bounded and unbounded CTB foundation over subgrade on the fatigue and erosion related distresses in concrete pavements. KENSLAB, an elaborate finite element program is used to determine the concrete pavement responses: stresses and deflection under the defined parameters. The results obtained using this software is relatively close to known theoretical Westergaard solutions. Several other findings related to pavement performance and behavior are made through this study. Multiple axle configurations is less damaging than single axle configuration in terms of fatigue life. Increasing the thickness is very effective in reducing the edge stress. Using concrete with higher modulus of elasticity brings only a small increase to the edge stress. Increasing the slab thickness is the most effective way to increase the fatigue life. Increasing subgrade modulus is more effective in reducing corner deflection than decreasing edge stress. The availability of tied shoulder construction gives significant impact in both reducing edge stress and corner deflection. The debonding condition between layers has a significant effect on pavement responses.

Keywords: Concrete pavement, fatigue failure, erosion failure, finite element, KENSLAB.

1 INTRODUCTION

1.1 Background

The most common failure modes that occur on concrete pavements are fatigue cracking at concrete slab and or erosion of materials in sub-layers. Both are related to excessive stresses and deflections on concrete pavement.

Many analytical models and solutions are provided by a large number of researchers to determine the mechanistic properties that occur on concrete pavement --- stresses and deflections. However, it is hardly possible to make analytical solutions for every boundary condition. Numerical models, such as finite element method offer the advantage of studying the effects of different parameters with minimal cost increase.

Huang in 1993 (which was then revised in 2004) developed KENSLAB, a simple and powerful finite element program which is made based on thin plate finite element resting on foundation. The program was made to address the responses of concrete pavement under several conditions. With this program, several loading conditions such as single axle load, tandem axle load and tridem axle load, or other design parameters that have been widely applied in concrete pavement construction, such as various concrete and subgrade properties, joint characteristics, slab thickness, application of shoulder construction, or application of additional material to concrete pavement construction, can be more accurately analyzed.

Although structural models can be modeled by several finite element programs, distress models of concrete pavement are mostly given in regression equations derived empirically with a large scatter data (Huang, 2004). One of the available models is the one given by Portland Cement Association (PCA) that provides distress models for both fatigue and erosion failure.

Using both structural model and distress model, the effect of applying different design parameters on concrete pavement behavior will be investigated within the study presented in this thesis.

1.2 Problem Statement

Research presented in this thesis aims to understand the effect of applying several parameters: different axle load configuration, concrete properties, subgrade properties, slab thickness, joint characteristics, shoulder construction, bonded Hot Mix Asphalt (HMA) overlay on concrete pavement, and bounded and unbounded Cement treated Base (CTB) foundation over subgrade on concrete pavement performance. The pavement behaviors that may lead to increase both fatigue and erosion failure as the

effect of applying each parameter will be computed and investigated.

1.3 Objectives

The objectives of this study are as follows:

a) To understand the mechanistic response of concrete pavement using finite element formulations;
b) To study and investigate the effect of different loading characteristics, material parameters, or other construction characteristics on concrete pavement structural responses related to fatigue and erosion failure;
c) To study and investigate the allowable load repetitions of concrete pavement under different loading characteristics, different application of material, or other construction characteristics.

1.4 Scope of Study and Limitations

Finite element formulations are computed using a computer program i.e. KENSLAB and allowable load repetitions are computed using empirical equations recommended by PCA. Sensitivity analysis is performed to analyze the structural performance of concrete pavement under different design parameters, as follows:

a) Loading: single, tandem, tridem axle load
b) Concrete modulus of elasticity
c) Modulus of subgrade reaction
d) Slab thickness
e) Dowel characteristic
f) Shoulder availability
g) HMA overlay over concrete pavement construction
h) Additional CTB Foundation

However, on account of time and resources constraints, this study is subjected to the following limitations:

a) The analysis only considers the effect of axle loading on concrete pavement. Thermal cracking is not accounted.
b) The type of concrete pavement to be analyzed is Jointed Plain Concrete Pavement (JPCP).
c) The loadings are assumed to be static.

2 LITERATURE REVIEW

2.1 Analytical Solution: Westergaard Formula

Westergaard (1947) proposed the first complete theory of structural behavior of concrete pavement. The analytical equations by Westergaard for corner loading and edge loading are given by:

Corner loading:

$$\sigma = \frac{3P}{h^2}\left[1 - \left(\frac{a\sqrt{2}}{\ell}\right)^{0.6}\right] \tag{1}$$

$$\Delta = \frac{P}{k\ell^2}\left[1.1 - 0.88\left(\frac{a\sqrt{2}}{\ell}\right)\right] \tag{2}$$

Edge loading:

$$\sigma = \frac{0.803P}{h^2}\left[4log\left(\frac{\ell}{a}\right) + 0.666\left(\frac{\ell}{a}\right) - 0.034\right] \tag{3}$$

$$\Delta = \frac{0.431P}{k\ell^2}\left[1 - 0.82\left(\frac{a}{\ell}\right)\right] \tag{4}$$

where σ is tensile stress, Δ is deflection, P is concentrated load, ℓ is the relative stiffness.

It has been virtually impossible to obtain analytical (closed-form) solutions for many pavement structures because of complexities associated with geometry, boundary conditions, and material properties. Since the existing analytical solutions are based on infinitely large slab with no discontinuities, they cannot in principle be applied to analysis of jointed or cracked slabs of finite dimensions, with or without load transfer systems at the joints and cracks (Darestani, 2007; Minnesota, 2003; Zhang et al, 2004).

2.2 Concrete Pavement Distresses

2.2.1 Fatigue damage of concrete slab

As the main reason behind deterioration processes, cracks can be considered as a tensile failure in concrete pavements. Cracks can occur at any location within the pavement where tensile stresses exceed the concrete flexural strength. Since the applied loads are repeatable in nature, concrete pavements fail under fatigue phenomenon rather than direct failure under maximum induced tensile stress. The fatigue of concrete can cause both transverse cracking, which initiates at the pavement edge midway between transverse joints, and longitudinal cracking, which initiates in the wheel path nearest the slab centerline (Huang, 2004). Figure 1 shows the most critical loading locations to be considered for fatigue analysis.

Because the loading is placed considerably far away from joints, the presence of dowel bar inside the transverse joint has practically no effect on pavement responses. Consequently, in the pavement modeling and analysis conducted particularly for this case, the presence of transverse joint at JPCP is neglected.

2.2.2 Erosion of subbase and subgrade materials

Pumping and erosion of material beneath and beside the slab is another main distress occurring at concrete pavement that needs to be counted in addition to fatigue cracking. Such distresses are related more to pavement deflection than flexural stress, which is the main issue contributing in fatigue distresses. Huang (2004) concluded that the most critical pavement deflection occurs at slab corner when axle load is placed at the joint near the corner, as shown in Figure 2.

2.2.3 Allowable load repetitions

The structural models for concrete pavement are more advanced than the distress models. Mechanistic analysis such as finite element methods can be used to build an appropriate structural model, but most of distress models are regression equations derived empirically with a large scatter of data (Huang, 2004).

According to Barenberg (2005), fatigue failure of concrete pavement is related to the ratios of applied stress to the concrete strength. Many distress models take the stress-strength ratio into consideration. Portland Cement Association (PCA) recommended the following equations for predicting the allowable number of load repetitions for fatigue failure on concrete pavement:

$$\text{For } \frac{\sigma}{S_c} \geq 0.55: log\, N_f = 11.737 - 12.707 \left(\frac{\sigma}{S_c}\right) \quad (5)$$

$$\text{For } 0.45 < \frac{\sigma}{S_c} < 0.55: \; N_f = \left(\frac{4.2577}{\frac{\sigma}{S_c} - 0.4325}\right) \quad (6)$$

$$\text{For } \frac{\sigma}{S_c} \leq 0.45: \; N_f = \text{unlimited} \quad (7)$$

where N_f is the allowable number of load repetitions for fatigue failure, σ is flexural stress in concrete slab, and S_c is modulus of rupture of concrete.

For erosion analysis, PCA recommended the equation below to determine the allowable load repetitions:

$$log\, N_e = 14.524 - 6.777(C_1 P - 9.0)^{0.103} \quad (8)$$

where N_e is the allowable load repetitions for erosion failure, C_1 is an adjustment factor (1 for untreated subbases and 0.9 for stabilized subbases), and P is the rate of power, defined by:

$$P = 268.7 \frac{p^2}{hk^{0.73}} \quad (9)$$

where p is the pressure on the foundation under the slab corner in psi, which is equal to kw for liquid foundation, where w is the maximum deflection, h is the thickness in inches, and k is the modulus of subgrade reaction in pci.
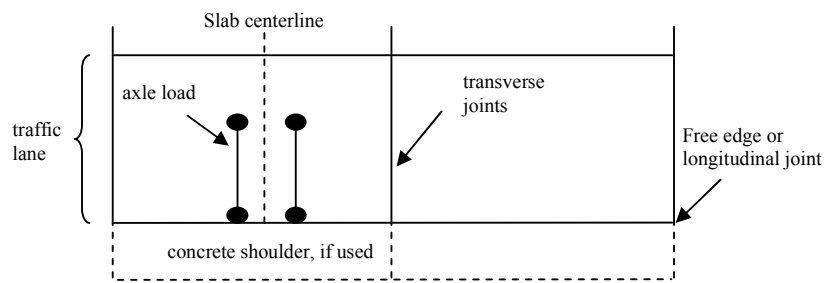
Figure 1. Most critical loading position for fatigue failure (Huang, 2004)
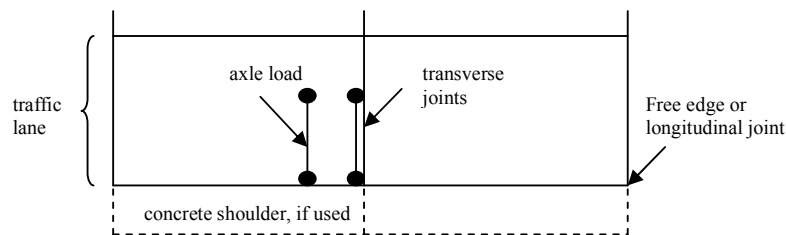
Figure 2. Most critical loading position for erosion failure (Huang, 2004)

3 THEORETICAL BACKGROUND

3.1 Finite Element Analysis

The finite element method enables the most accurate modeling of the real situation with respect to the external loadings, the geometry of the discontinuous concrete pavement, the material characteristics, and the interaction between the various layers of the pavement structure (Houben, 2006). So from finite element calculations, one can expect more detailed and more realistic data about stresses and deflections within a concrete pavement structure that can be obtained by means of the analytical methods. Several assumptions and considerations taken in finite element analysis using KENSLAB is discussed below.

3.2 Liquid Foundation

The liquid foundation is also known as Winkler foundation. It shows the force-deflection relationship which is characterized by an elastic spring. The stiffness of a liquid foundation is defined by:

$$k = \frac{p}{w} \qquad (10)$$

where: k is modulus of subgrade reaction; p is pressure or force per unit area; w is vertical deflection.
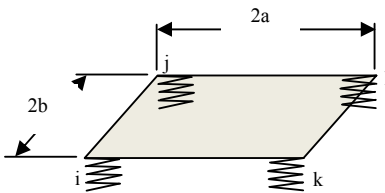
Figure 3. Liquid foundation under a plate element (Huang, 2004)

A large number of springs under a rectangular plate element, with a length of 2a and a width of 2b, are replaced by four identical springs at the corners. The force on each spring is equal to: the unit pressure p multiplied by the area a x b, From Equation 10, $p = kw$, so:

$$F_{wi} = kabw_i \qquad (11)$$

where F_{wi} = force at node i, w_i = deflection at node i.

3.3 Stiffness Matrix of Slab

Figure 4 shows a rectangular finite element with nodes $i, j, k,$ and l. There are three fictitious forces and three corresponding displacements at each node. Vertical force F_w, moment about the x axis $F_{\theta x}$, and moment about the y axis $F_{\theta y}$ are the three forces while

the three displacements consist of the vertical deflection in the z direction w, rotation about the x axis θ_x, and rotation about the y axis θ_y.
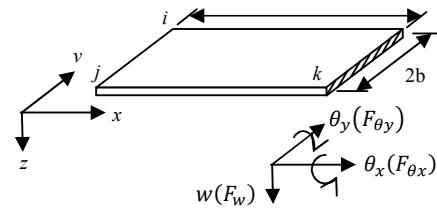
Figure 4. Rectangular finite element (Huang, 2004)

For each element, the forces and displacements are related by:

$$\begin{Bmatrix} F_i \\ F_j \\ F_k \\ F_l \end{Bmatrix} = \left[K_p\right]^e \begin{Bmatrix} \delta_i \\ \delta_j \\ \delta_k \\ \delta_l \end{Bmatrix} \qquad (12)$$

where $\left[K_p\right]^e$ = element stiffness matrix of a plate, F_i; F_j; F_k; F_l = forces at node $i, j, k,$ and l, and δ_i; δ_j; δ_k; δ_l = displacement at node $i, j, k,$ and l.

At any given node,

$$F_i = \begin{Bmatrix} F_{wi} \\ F_{\theta xi} \\ F_{\theta yi} \end{Bmatrix} \qquad \delta_i = \begin{Bmatrix} w_i \\ \theta_{xi} \\ \theta_{yi} \end{Bmatrix} \qquad (13)$$

By combining the stiffness matrixes of slab foundation and joint, and replacing the fictitious nodal forces with the statical equivalent of the externally applied wheel loads, a set of simultaneous equations is obtained for solving the unknown nodal displacements:

$$[K]\{\delta\} = \{F\} \qquad (14)$$

where $[K]$ is the overall stiffness matrix, $\{\delta\}$ are the nodal displacements, and $\{F\}$ are the externally applied nodal forces.

3.4 Two Layers of Slab

KENSLABS can have two layers of slab, either bonded or unbonded.

3.4.1 Bonded slabs

Figure 5 shows a composite pavement system, with the top layer having a thickness of h_1, an elastic modulus E_1, and a Poisson ratio v_1 that has been placed on a slab with a thickness h_2, an elastic modulus E_2, and a Poisson ratio v_2. The left figure is the original section with a unit width, and the right

figure is the equivalent section in which the width of hot mix asphalt is reduced to E_1 / E_2.

If the moment is taken at the bottom surface, the distance d from the neutral axis to the bottom of the slab is:

$$d = \frac{(E_1/E_2)h_1(0.5h_1 + h_2) + 0.5h_2{}^2}{(E_1/E_2)h_1 + h_2} \qquad (15)$$

The composite moment of inertia I_c about the neutral axis is:

$$I_c = \left(\frac{E_1}{E_2}\right)\left[\frac{1}{12}h_1{}^3 + h_1(0.5h_1 + h_2 - d)^2\right] + \frac{1}{12}h_2{}^3 \\ + h_2(d - 0.5h_2)^2 \qquad (16)$$

Given the moment M, the flexural stress f at the bottom of concrete slab is:

$$f = \frac{Md}{I_c} \qquad (17)$$

3.4.2 Unbonded slabs

If there is no bond between the two layers, each layer is considered an independent slab with the same displacements at the nodes. Therefore, the stiffness matrix of the slabs is the sum of the stiffness matrices of the two layers. After the displacements are determined, the moments at each node in each layer can be computed. After the moment M in each slab is found, the flexural stress f can be determined by.

3.4.3 Stiffness of joint

The stiffness of joint is represented by a shear spring constant C_w,

$$C_w = \frac{Shear\ force\ per\ unit\ length\ of\ joint}{Deflections\ difference\ between\ two\ slabs} \qquad (18)$$

In the finite element method, the shear forces are concentrated at the nodes along the joint. From Equation 18,

$$F_w = LC_w w_d \qquad (19)$$

F_w is the nodal force applied to both slabs through the springs and L is the average nodal spacing at joint. The forces F_w can then be substituted into Equation 13 to solve the nodal displacements.

When dowel bars are used to transmit shear, it is assumed that they are concentrated at the nodes. If the dowel spacing is s_b, the number of dowels at each node is L/s_b The force F_w is divided by the number of dowels needed to obtain the force P_t on each dowel:

$$P_t = \frac{s_b F_w}{L} \qquad (20)$$

The difference in deflection w_d is caused by the shear deformation of the dowel ΔS and the deformation of concrete under the dowel y_0:

$$w_d = \left(\frac{z}{GA} + \frac{2 + \beta z}{2\beta^3 E_d I_d}\right) P_t \qquad (21)$$

in which P_t is the shear force on one dowel bar, z is the joint width, A is the area of the dowel, and G is the shear modulus of the dowel, β is the relative stiffness of dowel.

Shear spring constant C_w for doweled joint is:

$$C_w = \frac{1}{s_b\left(\dfrac{z}{GA} + \dfrac{2 + \beta z}{2\beta^3 E_d I_d}\right)} \qquad (22)$$
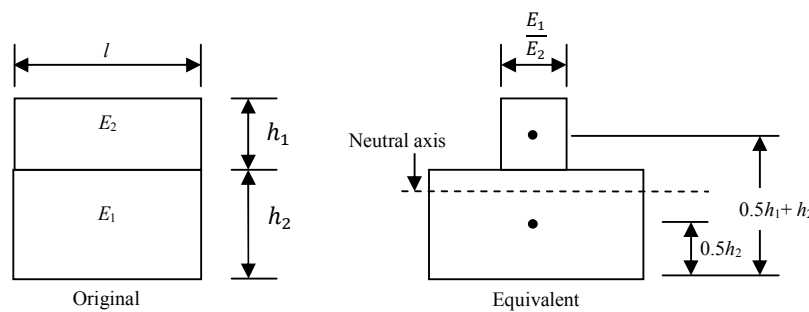
Figure 5. Original versus equivalent section of composite pavement (Huang, 2004)
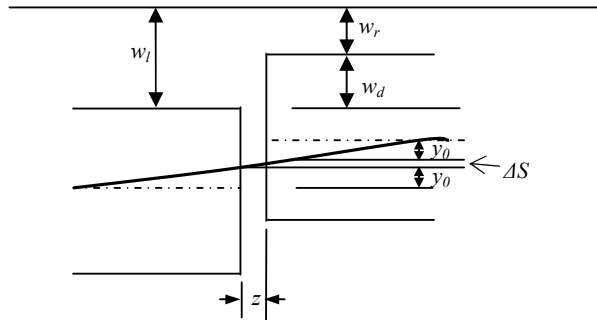
Figure 6. Shear transfer through joint by dowel bar
(Huang, 2004)

4 METHODOLOGY

4.1 General

Sensitivity analysis to investigate the effect of different parameters on concrete pavement performance was conducted using the computer program KENSLAB. Two different verifications, namely comparisons with Westergaard solutions and investigation of results obtained under different mesh size were performed to check the reliability of the finite element analysis using KENSLAB. Critical Allowable Load Repetitions were computed to determine the most critical failure possible to occur.

4.2 Axle Configuration

General configuration for single, tandem, and tridem axle load is used in this research. The single axle is a standard 80 kN axle with dual tires spacing of 35 cm. Each of the tandem and tridem axles is the same as the single axle, so in the end, the total load on tandem axles is 160 kN, and on tridem axles is 240 kN. The spacing between the two axles is 120 cm and the distance between centers of dual tires is 195 cm.

4.3 Contact Area

A 80 kN axle has two sets of dual tires where each dual tires has a load of 20 kN and contact pressure of 690 kPa.
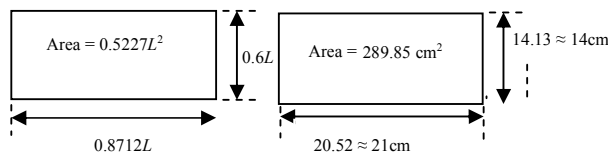
Figure 7. Tire Contact Area

The contact area is converted to a rectangular load with 21 cm in length and 14 cm in width.

4.4 Edge Loading Modeling

For edge loading modelling, slab with 500 cm long and 350 cm wide is used. Because of symmetrical

geometry, only one half slab, l=250 cm needs to be considered. Only half part of the axle set that is placed in one part of half slab is applied, as shown in Figures 8 to 9.
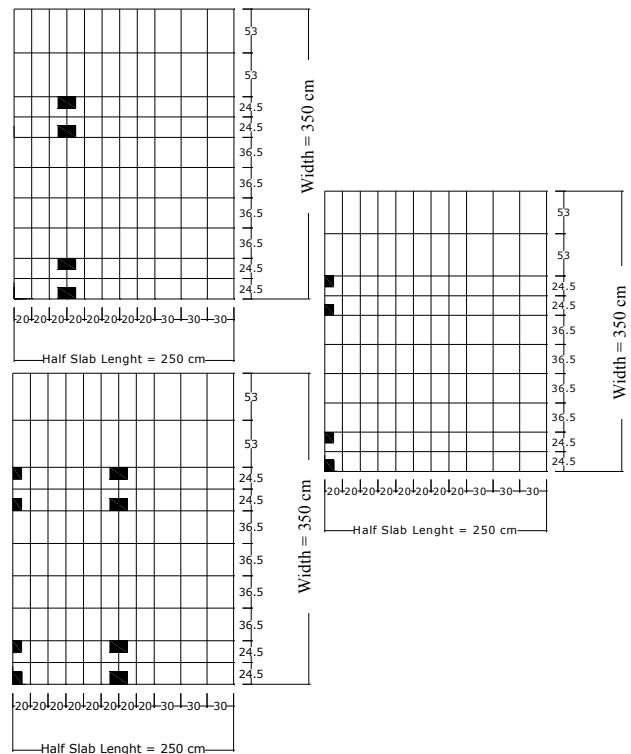
Figure 8. Mesh generation of edge loading analysis for single, tandem, and tridem axle configuration
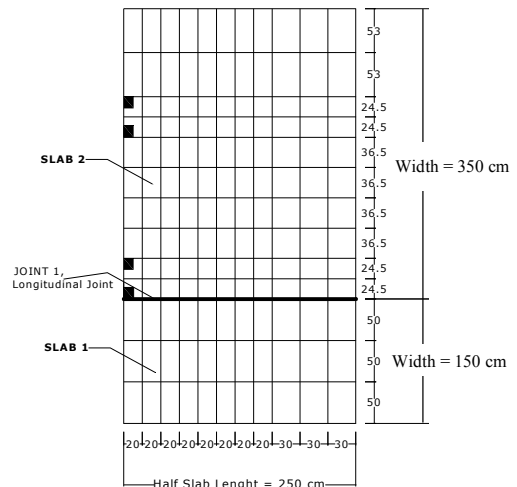
Figure 9. Mesh generation of edge loading analysis for singe axle configuration on concrete pavement with tied shoulder system

4.5 Corner Loading Modeling

For corner loading modelling, two slabs with 500 cm long and 350 cm wide each are used. These two slab constructions are tied with transversal joint. The front

axle loading is located at the corner of slab, near the transversal and longitudinal joint.
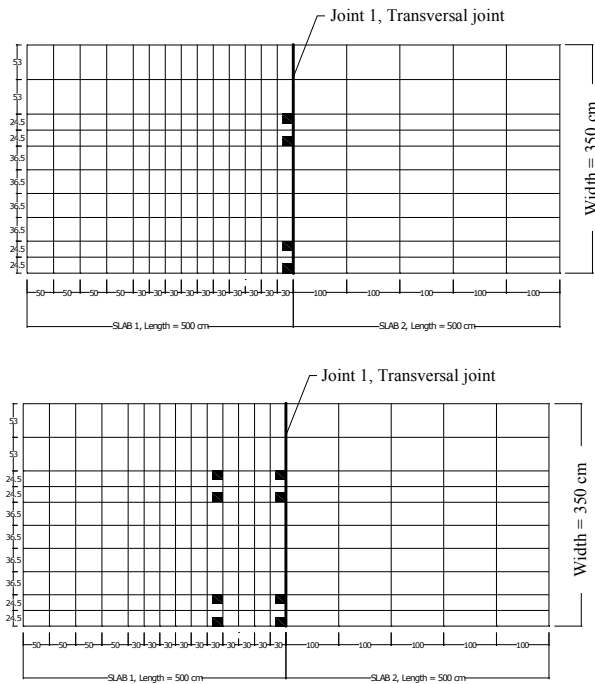
Figure 10. Mesh generation of corner loading analysis for single and axle configuration
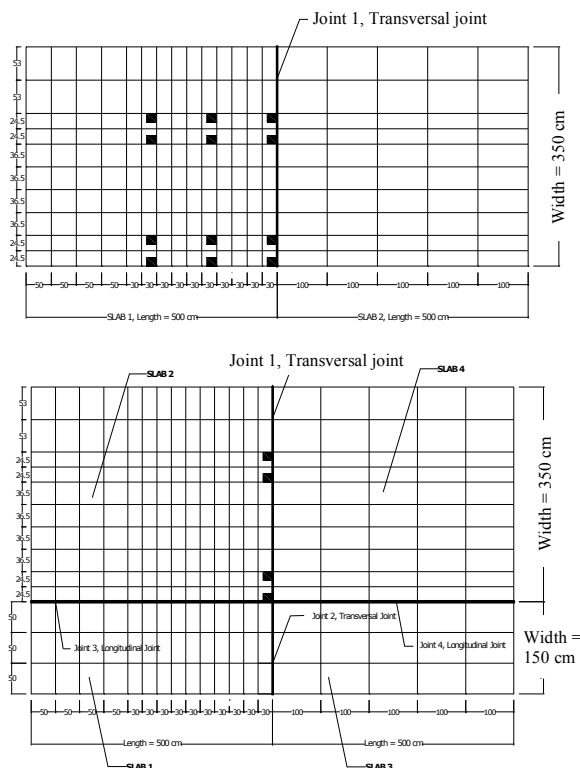
Figure 11. Mesh generation of corner loading analysis for tridem axle configuration and singe axle configuration on concrete pavement with tied shoulder system

5 RESULTS AND DISCUSSION

5.1 Comparison with Westergaard Solution

An evaluation was performed to verify the results obtained using KENSLAB and Westergaard formulas, which have been theoretically accepted. Two loading conditions, edge loading and corner loading were chosen, and the maximum tensile stresses and deflections obtained under those conditions were compared.

Westergaard presented generalized solutions for maximum stress and deflection that occurred on concrete slab with infinite length. In the finite element analysis, represented by KENSLAB, the conditions are approximated by a large slab, 10 m long by 10 m wide. Parameters used in this verification are:

Slab dimension:
Length x width = 1,000 cm x 1,000 cm
Slab thickness   : 25 cm
Modulus of Elasticity   : $E = 2.5 \times 10^7$ kPa
Poisson's Ratio   : $v = 0.15$
Modulus of subgrade reaction   :
$k = 27.1$ MN/m^3 (CBR = 3)
Both results obtained from different methods are checked very closely. The discrepancy of maximum stresses and maximum deflection are $\pm$ 3% or less and $\pm$ 6% or less, respectively.

5.2 Effect of Element Size

An analysis was performed on different mesh size to investigate the effect of element or mesh size on the concrete pavement responses obtained by using the finite element analysis. Three different models with different characteristics are used in this analysis, as follows:

a. High density mesh; consists of 13 nodes in x direction and 15 nodes in y direction
b. Medium density mesh; consists of 8 nodes in x direction and 11 nodes in y direction
c. Low density mesh; consists of 5 nodes in x direction and 8 nodes in y direction

The slab is subjected to 20 kN single wheel load loading, with tire pressure of 690 kPa. Other parameters used are similar to those stated in the previous section.

5.3 Edge Loading Analysis

Edge loading analysis is related to fatigue failure of concrete pavement. Therefore, the response that needs to be considered is the maximum tensile stress.

Table 1. Comparison of maximum stress and deflection computed using KENSLAB and Westergaard Equations

Wheel Load	Tire Pressure	Maximum Tensile Stress (kPa)			Maximum Deflection (mm)		
(kN)	(kPa)	Westergaard	KENSLAB	Discrepancy	Westergaard	KENSLAB	Discrepancy
EDGE LOADING							
20	690	1,075.5	1,106.9	-3%	0.265	0.263	1%
40	690	1,854.4	1,884.8	-2%	0.513	0.506	1%
2 x 20	690	1,088.0	1,101.6	-1%	0.491	0.460	6%
2 x 40	690	2,831.0	2,801.9	1%	0.942	0.885	6%
CORNER LOADING							
20	690	678.9	662.1	2%	0.656	0.689	-5%
40	690	1,227.9	1,198.7	2%	1.250	1.304	-4%
2 x 20	690	1,088.0	1,101.6	-1%	1.173	1.239	-6%
2 x 40	690	1,942.4	1,999.8	-3%	2.204	2.342	-6%

Table 2. Effect of mesh density on responses under edge loading

Mesh Density	Maximum Stress (kPa)	Dis-crepancy	Maximum Deflection (mm)	Dis-crepancy
High	1,106.9	0%	0.263	0%
Medium	1,045.7	5%	0.255	3%
Low	900.6	18%	0.217	18%
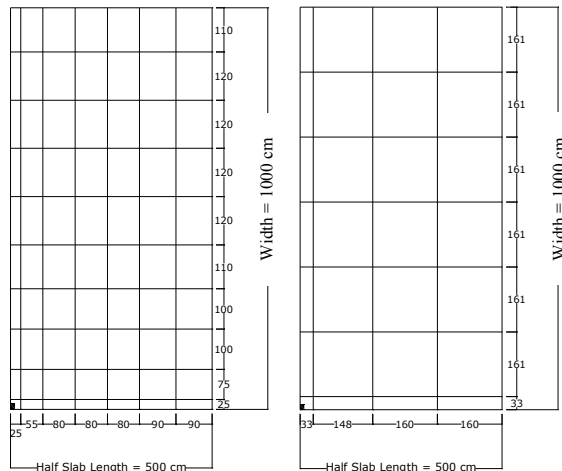
Figure 12. High, medium, and low density meshes

5.4 Base Case

The base case of edge loading analysis was used for analyzing the pavement performance subjected to single axle 80 kN load. The parameters used in the base case were:

Slab dimension:
Length x width = 1,000 cm x 1,000 cm
Slab thickness   : 25 cm
Modulus of Elasticity   : $E = 2.5 \times 10^7$ kPa
Poisson's Ratio   : $v = 0.15$

Modulus of subgrade reaction   : $k = 27.1$ MN/m^3
(CBR = 3)

Both results obtained from different methods are checked very closely. The discrepancy of maximum stresses and maximum deflection are ± 3% or less and ± 6% or less, respectively.
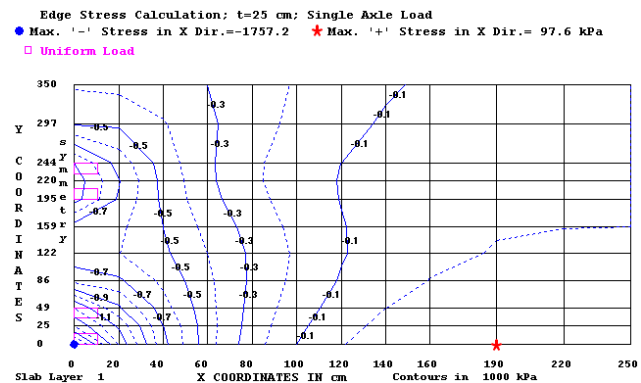
Figure 13. Stresses contour of slab under the base case

Figure 13 shows the contour of stress occurring when pavement is subjected to single axle load configuration. The maximum stress is 1757.191 kPa, and it occurs at the edge of the half slab, or at the center of concrete slab. In addition to this base case, another seven more cases as mentioned in the parametric study, each representing a different parameter from the base case, were also analyzed. Unless mentioned in certain cases below, the other parameters used in those cases were similar to the base case. Among the parametric studies are:

a) Loading: Tandem, Tridem axles load
b) Elastic modulus of concrete ( ): 3.0 E+7 kPa, 3.5 E+7 kPa

c) Modulus of subgrade reaction (*k*): 40.7 MN/m3; 54.3 MN/m3
d) Slab thickness: 27.5 cm; 30 cm
e) Shoulder availability: 1.5 m
   modulus of dowel support=407 GPa; modulus of steel=200 GPa; joint width=5mm; tie bar diameter=16 mm; and tie bar spacing=75 cm
f) HMA overlay on PCC
   E, v HMA   : 3.0 E+6 kPa; 0.35
   Thickness   : 10 cm
   Debonding Condition : bonded
g) Additional CTB foundation
   E, v CTB   : 1.0 E+7 kPa; 0.15
   Thickness   : 10 cm
   Debonding Condition: bonded and unbounded

Below is the result of investigation of the effect of different axle configuration on concrete pavement edge stresses. Other parametric studies are shown in Table 3.
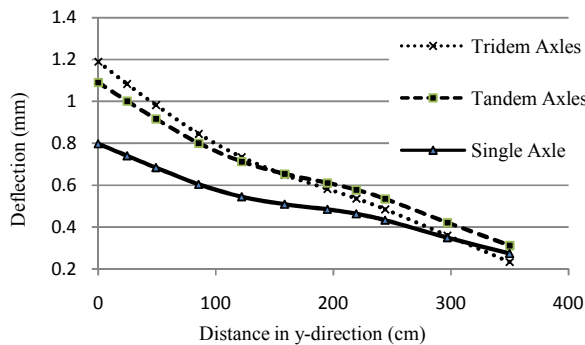
Figure 14. Effect of axle configuration on pavement stresses

5.5 Corner Loading Analysis

Corner loading analysis is related to erosion failure of concrete pavement. Maximum deflection was the main response that needs to be considered.

5.6 Base Case

The parameters used in the base case are:

Load	: single axle load
Slab thickness	: 25 cm
Layers (from top to bottom)	: Concrete slab; subgrade
Slab dimension	: 500 cm x 350 cm
Modulus of Elasticity of concrete	: $E = 2.5 \times 10^7$ kPa
Poisson's Ratio	: $v = 0.15$
Modulus of subgrade reaction	: $k = 27.1$ MN/m^3 (CBR = 3)
Modulus of	: 407 GPa

dowel support (k)

Modulus of steel	: 200 GPa
Joint width	: 5mm
Dowel diameter	: 32 mm
Dowel spacing	: 30 cm

Figure 15 shows the deflection at the pavement when it was subjected to loading and parameters used in the base case. The maximum deflection was 0.7971 mm and it occurred at the slab corner. The deflection decreased along with the distance away from the corner.

In addition to this base case, another eight more cases, each representing a different parameter from the base case, were also analyzed.

Figure 15. Deflection occurs at pavement subjected to single axle load due to corner loading

The parameter of each case is similar to the parameter of edge loading analysis. One more case is also included in the corner analysis: the effect of dowel characteristics. It is conducted by applying different parameters than that which has been analyzed in the base case: changing dowel spacing to 15 cm and installing 48 mm diameter dowel bar.

Below is the result of investigation of the effect of different axle configuration on concrete pavement deflections. Other parametric studies are shown in Table 3.
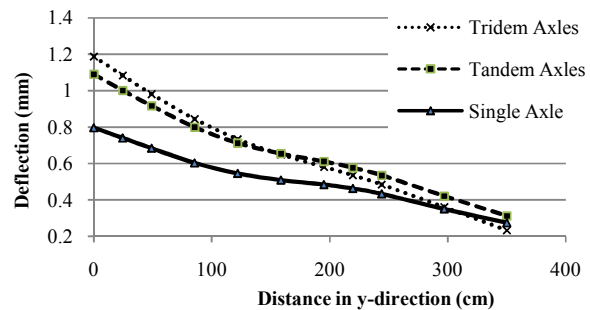
Figure 16. Effect of axle configuration on pavement deflections

5.7 Summary of Parametric Studies

The sensitiveness of different parameters on concrete pavement responses, as the result of investigation conducted for both fatigue and erosion analysis, are shown in Table 3. Unless mentioned in certain cases below, in consequence of investigating the effect of application of certain parameter on concrete pavement performance, the other parameters used in those cases were similar to the base case.

5.8 Allowable Load Repetitions

This analysis is performed to study the most critical type of failure, due to different design parameters. The allowable load repetitions were computed based on PCA method for both fatigue analysis and erosion analysis. For the value of ratio of maximum stress and modulus of rupture (σ/Sc) ≤ 0.45, PCA assumes that the allowable number of load repetitions is unlimited.

Predicted allowable load repetition was determined by the most critical value obtained from fatigue and erosion analysis. If both the allowable number of load repetitions for both fatigue and erosion failure were considered to be unlimited, then the most critical value for the particular parametric studies could not be defined. As shown in Table 4, the most critical failure in each case was fatigue failure. The erosion failure happened when pavement was subjected to multiple axles loading

6 CONCLUSIONS

a) KENSLAB software, which is based on finite element method, is theoretically correct. The results obtained using this software is relatively close to known theoretical Westeergaard solutions.

b) The size of finite element mesh has a significant effect on the results obtained. Finer mesh will lead to more critical results. Selection of an appropriate mesh therefore requires careful consideration.

c) Multiple axle configuration is less damaging than single axle configuration in terms of fatigue life of concrete pavement, considering that it makes a lower edge stress compared to single axle loading. In contrast, multiple axle configuration contributes more in increasing corner deflection, which consequently increases the probability of erosion failure. Compared to the application of 80 kN single axle load, the use of tandem axle load and tridem axle load decreases the edge stress by 5% and 19%, but increases the corner deflection by 37% and 49%, respectively.

d) Using concrete with higher modulus of elasticity brings only a small increase to the edge stress, but on the contrary, it reduces the corner deflection. Increasing modulus of elasticity of concrete by 20% and 40% increases the edge stress by 3% and 5%, but decreases the corner deflection by 5% and 9%.

e) Increasing the slab thickness is the most effective way to increase fatigue life. Conclusion can be made by investigation conducted of the effect of applying different parameters to reduce the edge stress, as follows:

- Increasing slab thickness from 25 cm to 27. 5 cm and 30 cm decreases the edge stress by 14% and 25% respectively
- Increasing modulus of subgrade reaction by 50% and 100%, from 27.1 MN/m3 (equal to CRW value = 3) to 40.7 MN/m3 (CBR = 5.5) and 54.3 MN/m3 (CBR = 10) only decreases edge stress by 7% and 11%.
- Applying 10 cm CTB as unbounded layer which represents the function of CTB as an additional base course, only decreases the edge stress by 2%.
- Applying 150 cm shoulder decreases the edge stress by 13%. The decrease of the stress to that level can be achieved by simply increasing the slab thickness by 2.5 cm, which efficiently saves the amount of concrete needed by 76%.
- Applying 10 cm HMA overlay decreases the edge stress by 12%

f) Increasing modulus of subgrade reaction is more effective in reducing corner deflection than in decreasing edge stress. Increasing modulus of subgrade reaction by 50% and 100%, from 27.1 MN/m^3 (equal to CBR value = 3) to 40.7 MN/m^3 (CBR = 5.5) and 54.3 MN/m^3 (CBR = 10) decreases the corner deflection by 23% and 36%, but only decreases edge stress by 7% and 11%.

g) Increasing slab thickness is not as effective in reducing the corner deflection as it is in reducing the edge stress. Increasing slab thickness from 25 cm to 27. 5 cm and 30 cm decreases the edge stress by 14% and 25% respectively, but only decreases the corner deflection by 8% and 14%.

h) Increasing dowel spacing and dowel diameter does not give significant impact in reducing corner deflection.

i) In multilayer concrete pavement, the debonding conditions between layers have a significant effect on pavement responses. Unbonded 10 cm CTB layer decreases the edge stress by only 2%, while bonded 10 cm CTB layer decreases the edge stress by 52%.

j) The availability of tied shoulder construction gives a significant impact in both reducing edge stress and corner deflection. 150 cm tied shoulder construction can reduce the edge stress and corner deflection by 14% and 20% respectively.

Table 3. Sensitivity analysis of concrete pavement responses under several parameters

No	Case	Parameter Ratio	FATIGUE ANALYSIS		EROSION ANALYSIS	
			Maximum Stress (kPa)	difference	Maximum Deflection (w) (cm)	difference
i	Base Case		1,757,191	0%	0.7971	0%
	SENSITIVITY ANALYSIS:					
1	Loading					
	Tandem Axle Loads	2.0	1,676,294	-5%	1.0914	37%
	Tridem Axle Loads	3.0	1,428,306	-19%	1,1893	49%
2	Concrete Modulus:					
	E = 3,000 MPa	1.2	1,809,284	3%	0.7566	-5%
	E = 3,500 MPa	1.4	1,852,367	5%	0.7245	-9%
3	Subgrade Modulus:					
	k = 40.7	1.5	1,639,587	-7%	0.6107	-23%
	k = 54.3	2.0	1,556,837	-11%	0.5070	-36%
4	Slab Thickness:					
	t = 27.5 cm	1.1	1,519,098	-14%	0.7351	-8%
	t = 30 cm	1.2	1,325,328	-25%	0.6844	-14%
5	Joint Construction					
	dowel spacing = 15 cm	-	1,757,191	0%	0.7782	-2%
	dowel diameter =48 mm	-	1,757,191	0%	0.7775	-2%
6	with shoulder	-	1,522,195	-13%	0.6341	-20%
7	HMA+PCC					
	HMA 10cm	-	1,545,556	-12%	0.7423	-7%
8	PCC+CTB 10 cm					
	unbonded CTB	-	1,720,154	-2%	0.7910	-1%
	bonded CTB	-	845,754	-52%	0.6733	-16%

Table 4. Allowable load repetitions for different parameters

No	Case	Allowable Load Repetitions		Critical Allowable Load Repetitions	
		Fatigue failure (N_f)	Erosion failure (N_e)	Load (N)	Type of failure
i	Base Case	7.33E+05	3.54E+08	7.33E+05	Fatigue
	SENSITIVITY ANALYSIS:				
1	Loading				
	Tandem Axle Loads	2.82E+06	1.21E+06	1.21E+06	Erosion
	Tridem Axle Loads	unlimited	6.22E+05	6.22E+05	Erosion
2	Concrete Modulus:				
	E = 3,000 MPa	unlimited	unlimited	-	-
	E = 3,500 MPa	unlimited	unlimited	-	-
3	Subgrade Modulus:				
	k = 40.7 kN/m3	6.65E+06	1.13E+09	6.65E+06	Fatigue
	k = 54.3 kN/m3	2.70E+08	3.03E+09	2.70E+08	Fatigue
4	Slab Thickness:				
	t = 27.5 cm	1.04E+13	unlimited	1.04E+13	Fatigue
	t = 30 cm	unlimited	unlimited	-	-
5	Joint Construction				
	dowel spacing = 15 cm	7.33E+05	unlimited	7.33E+05	Fatigue
	dowel diameter =48 mm	7.33E+05	unlimited	7.33E+05	Fatigue
6	with shoulder	2.88E+11	unlimited	2.88E+11	Fatigue
7	HMA+PCC				
	HMA 5cm	2.80E+06	unlimited	2.80E+06	Fatigue
	HMA 10cm	8.16E+08	unlimited	8.16E+08	Fatigue
8	PCC+CTB 10 cm				
	unbonded CTB	1.27E+06	8.72E+08	1.27E+06	Fatigue
	bonded CTB	unlimited	unlimited	-	-

k) As indicated in the allowable load repetitions computations using PCA method, single axle load configuration is more critical in fatigue analysis, while multiple axles configuration is more critical in erosion analysis.

7   RECOMMENDATIONS

a) The loads are assumed to be static, although they are acting dynamically in the nature. It is recommended to further analyze the behavior of concrete pavement by also considering the vehicle speed.
b) The result of finite element analysis should also be countered with the actual field investigation. Further calibration with actual field observation will give a significant development of finite element analysis of concrete pavement.
c) The effect of thermal condition on concrete pavement is also one of the major factors contributing to pavement failure. Taking this variable into account will simulate the actual condition of concrete pavement more precisely.
d) The fully bonded and unbonded conditions give a very different response of concrete pavement. In reality, the actual debonding conditions between concrete slab and concrete subbase (such as CTB) can be partially bonded. It is recommended to study this behavior in the future.

REFERENCES

Barenberg, E. (2005). "Factors Affecting Fatigue Failure of Concrete." *Proceeding on Workshop on Fracture Mechanics for Concrete Pavements: Theory to Practice*. Colorado, USA.

Darestani, M.Y. (2007). *Response of Concrete Pavements Under Moving Vehicular Loads and Environmental Effects*. Quensland University of Technology, Australia.

Houben, L.J.M. (2006). *Structural Design of Pavements, Part IV: Design of Concrete Pavements,* Lecture Notes. Faculty of Civil Engineering and Geosciences, TU-Delft The Netherlands.

Huang, Y. H. (1993). *Pavement Analysis and Design.* Prentice Hall, Englewood Cliffs, NJ.

Huang, Y.H. (2004). *Pavement Analysis and Design*, Second Edition. Prentice Hall, New Jersey.

Minnesota, (2002). *Load Testing of Instrumented Pavement Sections*. University of Minnesota, USA.

Westergaard, H. M., (1947). "New Formulas for Stresses in Concrete Runways of Airports." *ASCE Proceedings* 113, ASCE

Zhang, Z., Kawa, I., Hudson, W.R. (2004). "Impact of Changing Traffic Characteristics and Environmental Conditions on Performance of Pavements." *Center for Transportation Research Report*, The University of Texas at Austin, USA.